iScience

CellPress
OPEN ACCESS

Article

Performance of ^{18}F-FDG PET/MRI and its parameters in staging and neoadjuvant therapy response evaluation in bladder cancer

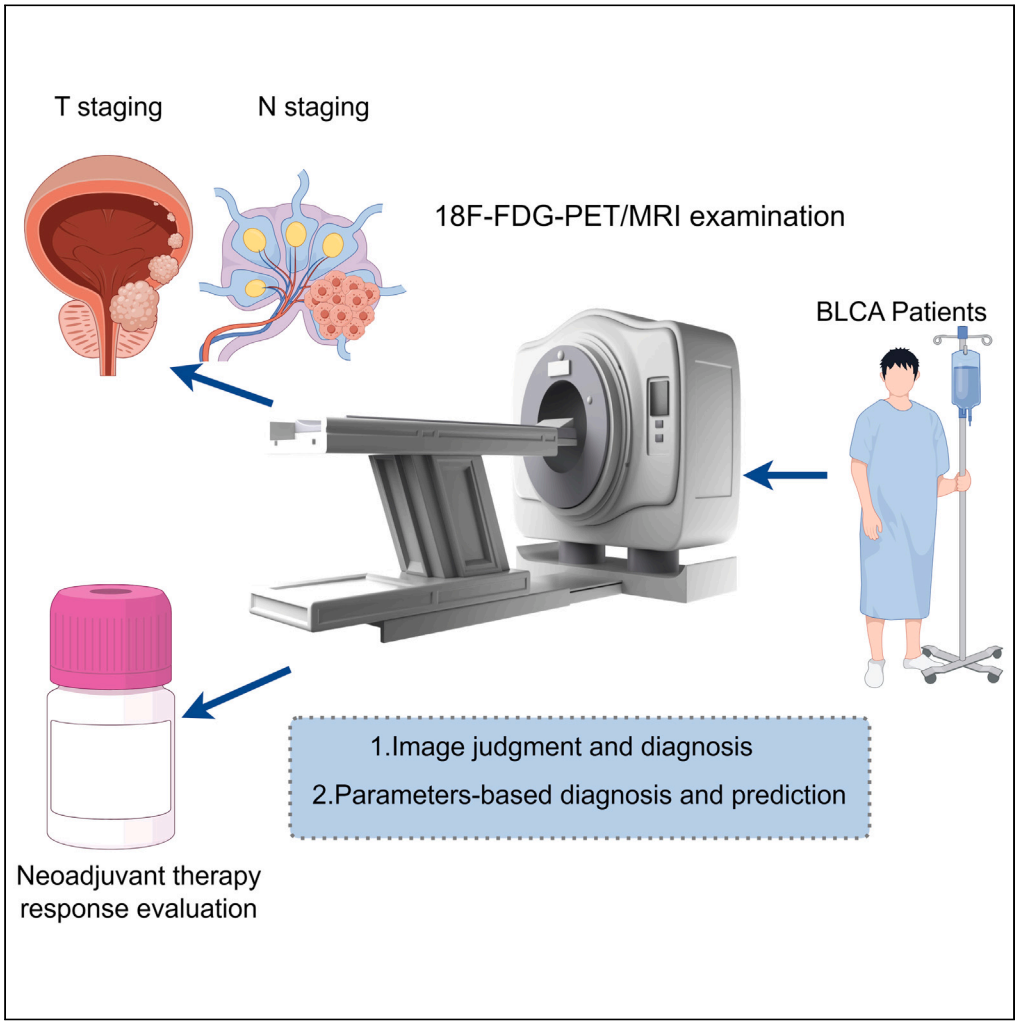

Tianhang Li, Qinqin You, Shiwei Zhang, ..., Shuyue Ai, Rong Yang, Hongqian Guo

asy331@sina.com (S.A.)
doctoryr@gmail.com (R.Y.)
dr.ghq@nju.edu.cn (H.G.)

Highlights

^{18}F-FDG PET/MRI is a feasible imaging tool for BLCA T staging

^{18}F-FDG PET/MRI is useful in lymph node metastasis detection for BLCA

^{18}F-FDG PET/MRI performs well in evaluating and predicting the NAT response in BLCA

ΔSUVmean is a promising candidate biomarker for NAT response prediction

Li et al., iScience 27, 109657
May 17, 2024
https://doi.org/10.1016/j.isci.2024.109657

iScience

CellPress
OPEN ACCESS

Article

Performance of ^{18}F-FDG PET/MRI and its parameters in staging and neoadjuvant therapy response evaluation in bladder cancer

Tianhang Li,[1,2,3,6] Qinqin You,[4,6] Shiwei Zhang,[1,6] Rushuai Li,[4] Shangxun Xie,[1] Danyan Li,[5] Shuyue Ai,[4,*] Rong Yang,[1,7,*] and Hongqian Guo[1,*]

SUMMARY

^{18}F-FDG PET/MRI shows potential efficacy in the diagnosis of bladder cancer (BLCA). However, the performance of ^{18}F-FDG PET/MRI in staging and neoadjuvant therapy (NAT) response evaluation for BLCA patients remains elusive. Here, we conduct this study to evaluate the performance of ^{18}F-FDG PET/MRI and its derived parameters for tumor staging and NAT response prediction in BLCA. Forty BLCA patients were retrospectively enrolled to evaluate the performance of ^{18}F-FDG PET/MRI in staging and NAT response prediction in BLCA. The feasibility of using 18F-FDG PET/MRI-related parameters for tumor staging and NAT response evaluation was also analyzed. In conclusion, ^{18}F-FDG PET/MRI is found to show good performance in the BLCA staging and NAT response prediction. Moreover, ΔSUVmean is an efficacious candidate parameter for NAT response prediction. This study highlights that ^{18}F-FDG PET/MRI is a promising imaging approach in the clinical diagnosis and treatment for BLCA.

INTRODUCTION

Bladder cancer (BLCA) is a highly prevalent global malignancy, with 83,730 estimated new cases and 31,940 estimated related new deaths occurring in the United States in 2021.[1] The process of staging, utilizing the tumor, node, metastasis (TNM) system, plays a critical role in distinguishing non-muscle-invasive bladder cancer (NMIBC) (≤pT1) from muscle-invasive bladder cancer (MIBC) (≥pT2) and subsequently determining appropriate clinical interventions.[2,3] NMIBC is typically managed through transurethral resection of bladder tumor (TUR-BT) accompanied by adjuvant intravesical therapy.[4,5] The standard of care for muscle-invasive bladder cancer (MIBC) involves radical cystectomy (RC) followed by pelvic lymph node dissection (PLND).[2] Consequently, the importance of precise TNM stage assessment for BLCA using preoperative imaging techniques is inherently apparent.

Among the conventional imaging techniques, computed tomography (CT) has exhibited limited effectiveness in the clinical staging of BLCA.[6] In contrast, magnetic resonance imaging (MRI) has shown superior performance in local staging of BLCA, primarily owing to its enhanced soft tissue contrast.[7] Nevertheless, MRI lacks precision in accurately monitoring lymph node metastasis precisely,[7,8] thereby restricting its utility in BLCA staging. Positron emission tomography (PET)/MRI, a novel imaging method that combines the high resolution of MRI in primary tumor imaging and the high sensitivity of PET for monitoring lymph node metastasis, has demonstrated significant potential for staging various cancers.[9] However, the clinical feasibility of PET/MRI for diagnosing BLCA has been scarcely explored, with only a limited number of studies conducted thus far. Recently, Eulitt et al. investigated the efficacy of ^{18}F-FDG PET/MRI in primary tumor and lymph node metastasis detection in BLCA.[10] Nevertheless, limited by the small sample size of patients with true pathologic lymph node involvement, the role played by ^{18}F-FDG PET/MR in the staging of BLCA warrants further study.

Recently, neoadjuvant therapies by combining chemotherapy and immunotherapy for MIBC have exhibited significant effectiveness in reducing tumor size, thereby potentially enhancing prognosis of patients.[11,12] Several clinical trials focusing on neoadjuvant therapy (NAT) have revealed that a complete response (CR) could be achieved in certain individuals with BLCA.[13–15] Given the considerable morbidity associated with radical cystectomy (RC), patients who attain a CR may be able to forgo local treatment and

[1]Department of Urology, Affiliated Nanjing Drum Tower Hospital, Medical School of Nanjing University, Nanjing, China
[2]Department of Urology, Zhongda Hospital, Southeast University, Nanjing, China
[3]Surgical Research Center, Institute of Urology, Southeast University Medical School, Nanjing, China
[4]Department of Nuclear Medicine, Nanjing First Hospital, Nanjing Medical University, Nanjing, China
[5]Department of Radiology, Nanjing Drum Tower Hospital, Affiliated Medical School of Nanjing University, Nanjing, China
[6]These authors contributed equally
[7]Lead contact
*Correspondence: asy331@sina.com (S.A.), doctoryr@gmail.com (R.Y.), dr.ghq@nju.edu.cn (H.G.)
https://doi.org/10.1016/j.isci.2024.109657

Table 1. Baseline characteristics of the enrolled patients

Characteristic	n (%)
Median age at diagnosis, y (range)	73.5 (47–88)
Sex	
Male	32 (80)
Female	8 (20)
T stage	
T1 (NMIBC)	9 (22.5)
T2-3 (MIBC)	31 (77.5)
Grade	
Low	7 (17.5)
High	33 (82.5)
Lymph node metastasis	
Yes	5 (12.5)
Histology (Predominant)	
Urothelial carcinoma	40 (100)
Neoadjuvant treatment	
Yes	17 (42.5)

experience improved quality of life and survival outcomes. Identifying patients who do not benefit from NAT in a timely manner and discontinuing treatment earlier is crucial to prevent delays in the opportunity for surgery. Post-NAT TUR-BT is a commonly used approach to restage BLCA tumors and assess the effectiveness of NAT. However, TUR-BT is an invasive method that carries a significant risk of downstaging and cannot provide an accurate evaluation of NAT response.[16–18] Therefore, there is an urgent need for a more precise predictive tool to assess the response to NAT. PET/MRI has recently been employed in various cancers to evaluate the response to NAT.[19–21] In the case of BLCA, Salminen et al. conducted a study to assess the potential of ^{11}C-acetate PET/MR in predicting the response to neoadjuvant chemotherapy (NAC) and reported three accurate staging results out of five patients.[22] However, due to the limited sample size, the effectiveness of PET/MRI as a tool for predicting the responsiveness to NAT remains uncertain. Furthermore, there is currently a lack of studies investigating the efficacy of FDG-related nuclide imaging in BLCA.

Hence, we sought to assess the feasibility of ^{18}F-FDG PET/MRI in tumor staging and NAT response evaluation. Furthermore, we aimed to explore the potential of utilizing derived parameters from ^{18}F-FDG PET/MRI as supplementary diagnostic biomarkers for both staging and predicting the response to NAT.

RESULTS

Patients' clinical characteristics

The patients' clinical characteristics are listed in Table 1. The median age (year) was 73.5, ranging from 47 to 88. Thirty-two (80%) of the patients were male. The WHO/ISUP grading distribution was as follows: high grade, 33 (82.5%); low grade, 7 (17.5%). With regards to TNM stage based on the final specimens, 9 (22.5%) were NMIBC (pT $\leq$ T1), and 31 (77.5%) were MIBC (pT $\geq$ T2). Five (12.5%) patients were pathologically proven to have lymph node metastasis. 16 patients underwent only PET/MRI examination and TUR-BT treatment; 7 patients underwent PET/MRI scanning, TUR-BT, and RC + ePLND without NAT; 17 patients with histologically proven $\geq$ pT2 stage underwent NAT treatment. All the primary tumors were urothelial cancer and showed positive uptake of ^{18}F-FDG. For the patients who only underwent the TUR-BT surgery, the scope of electrosection was sufficient and there was no residual tumor at tumor base, which ensured the acquisition of relatively accurate staging results. Of the 17 patients with NAT, 12 received PET/MRI scanning twice before and after NAT, 4 missed the second PET/MRI scan, and 1 missed the first PET/MRI scan due to different unavoidable reasons. The flow chart of the protocol is shown in Figure 1.

Performance of ^{18}F-FDG-PET/MRI in tumor primary staging

The sensitivity, specificity, accuracy, and AUC (95% confidence interval) of ^{18}F-FDG-PET/MRI for the detection of MIBC were 0.967, 0.889, 0.949 and 0.928 (0.801–1.0), respectively (Table 2). Specifically, 30 patients were detected as $\geq$ T2, of which 29 patients were proved as true-positive MIBC patients and the other 1 patient was false-positive. Meanwhile, 9 patients were staged as NMIBC by ^{18}F-FDG-PET/MRI, of which 8 were pathologically proved as true-negative while the remaining 1 patient was proved as false-negative. Representative cases of radiological detection of MIBC and NMIBC are shown in Figures 2 and 3. The PET/MRI scanning results for individual patients are listed in Table 3. Of the 24 patients who underwent RC and ePLND, 5 (20.8%) were positive for lymph node metastasis. The sensitivity, specificity,

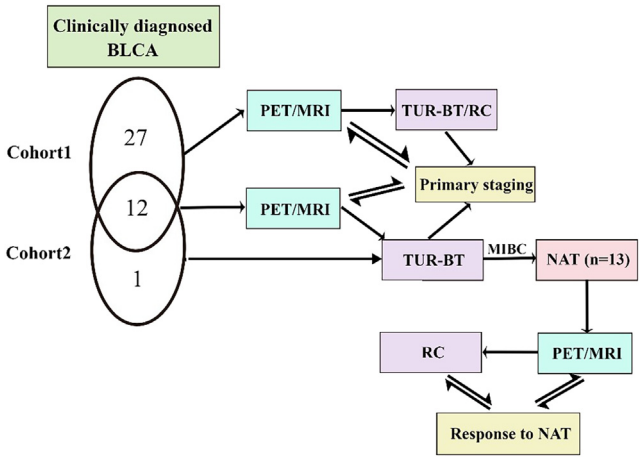

Figure 1. Flow chart of the study protocol

The study consisted of two cohorts. Cohort1: Accuracy of ^{18}F-FDG PET/MRI was evaluated on 39 treatment naive patients before any intervention of primary tumor. Cohort 2: treatment response to NAT was evaluated in 13 patients undergoing ^{18}F-FDG PET/MRI before TUR-BT and after NAT. Twelve patients participated in both cohorts of the study. In total, forty patients were enrolled.

accuracy, and AUC (95% confidence interval) of ^{18}F-FDG PET/MR for the detection of lymph node metastases were 80%, 89.5%, 87.5% and 0.806 (0.564–1), respectively (Table 4). Representative images of nodal involvement are shown in Figure 4.

Correlations between ^{18}F-FDG PET/MR derived parameters and pathological characteristics of BLCA

To investigate the potential diagnostic value of the parameters derived from ^{18}F-FDG PET/MR for discriminating different pathological characteristics of BLCA, we derived a range of parameters, including SUVmax, SUVmean, maximal tumor diameter and ADCmean, from the ^{18}F-FDG PET/MR images. Notably, metabolic tumor volume (MTV) and total lesion glycolysis (TLG) are only measurable and obtainable in only 4 patients due to the limitations in measurement tools. Therefore, we did not include MTV and TLG in the parameters. The values of the parameters were compared with different pathological characteristics. For pT stage, maximal tumor diameter (pT $\geq$ T2 vs. pT $\leq$ T1, p = 0.0415) and ADCmean (pT $\geq$ T2 vs. pT $\leq$ T1, p = 0.0041) differed significantly between the T2-T3 group and the T1 group (Table 5; Figures 5A and 5B). For pathological tumor grade, no significant difference was found between the low-grade and the high-grade groups for all the four parameters. Also, no significant difference was found between the N0 and N1 groups, possibly due to the low number of cases. Notably, the N1 group showed higher average values of maximal tumor diameter than N0 group but without a significant statistical difference (56.00(41–77) vs. 42.63(12–69), p = 0.1174). For pT stage, maximal tumor diameter and ADCmean could effectively differentiate NMIBC and MIBC with AUCs of 0.838 and 0.833, respectively (Figures 5C and 5D). In addition, the urine uptake values in PET of the BLCA patients are shown in Table S1.

Performance of ^{18}F-FDG PET/MR in NAT response prediction

Seventeen patients with pathologically proven MIBC underwent NAT therapy, of whom 12 patients received PET/MR scanning twice before and after NAT and 1 patient received PET/MR examination once after NAT. These 13 patients were enrolled to evaluate the performance of ^{18}F-FDG PET/MR in NAT response prediction. The histological results of the surgical specimen were regarded as the gold standard. A comparison between PET/MR results and pathological results is listed in Table 6. 11 out of the 13 (84.6%) were correctly staged by ^{18}F-FDG PET/MR examination. 1 patient was understaged, and 1 patient was overstaged. Typical response detection is demonstrated in Figures 6 and 7.

Correlations between the changes of PET/MRI-derived parameters before and after NAT and response to NAT therapy for bladder cancer patients

To explore whether the changes of the derived PET/MRI parameters before and after NAT could be utilized to evaluate and predict the response to NAT therapy for BLCA patients. We extracted the absolute value of the changes of the PET/MRI parameters during the NAT process, which are termed as Δdiameter, ΔSUVmean and ΔSUVmax. The patients were divided into two groups as the positive-response group and the negative-response group based the NAT response. The positive response is referred to that the post-NAT tumor is down-staged into NMIBC (pT $\leq$ T1) while the negative-response group is referred to that the post-NAT tumor remained the stage of MIBC (pT $\geq$ T2). Based on the differed NAT response for the BLCA patients who belonged to this cohort, we found that the value of ΔSUVmean showed a significant difference between the positive-response group and negative-response group (4.259 (1.655–8.050) vs. 0.7539(-2.280–3.043),

Table 2. Performance of T staging by PET/MR

Primary Tumor				
Gold standard from surgical specimens				
PET/MRI		Positive	Negative	In total
	Positive	29	1	30
	Negative	1	8	9
	In total	30	9	39
	Sensitivity	96.7%		
	Specificity	88.9%		
	PPV	96.7%		
	NPV	88.9%		
	Accuracy	94.9%		

p = 0.0241), ΔdiameterandΔSUVmax didn't show significant differences (Table 7). ΔSUVmean could effectively differentiate the positive-response and negative response patients for NAT therapy with the AUC (95% confidence interval) of 0.886 (0.689–1) (Figure 8).

DISCUSSION

The integration of PET, known for its high sensitivity in detecting lymph node metastases and visualizing tumor response to NAT, with MRI, which can accurately assess the extent of muscle infiltration in BLCA, offers significant potential in aiding the diagnosis of BLCA and evaluating the response to NAT. However, relevant studies still lacked. This current clinical investigation represents the inaugural study to comprehensively evaluate the performance and feasibility of ^{18}F-FDG-PET/MRI in tumor staging and NAT response prediction for BLCA.

As with the routine staging process for BLCA, cystoscopy, biopsy, and bimanual pelvic examination continue to be the gold standard for diagnosing and initially staging BLCA. Following confirmation of the diagnosis, imaging techniques such as computed tomography (CT) or magnetic resonance imaging (MRI) may be necessary to assess local disease staging, identify any synchronous lesions in the upper urinary tracts, determine nodal staging, and detect distant metastases. The routine staging process for BLCA begins with the evaluation of the emerged typical symptoms. Painless hematuria and frequency of urination are the most common symptoms, while the obstruction and

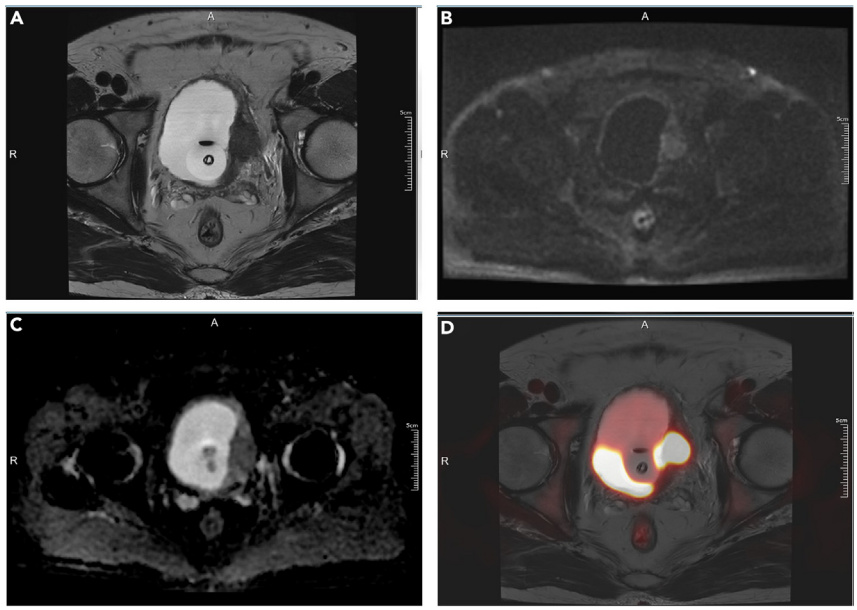

Figure 2. Pre-radical cystectomy ^{18}F-FDG PET/MRI images of a 66-year-old man

(A–D) The image shows a heterogeneous mass on the left wall of the bladder with an extension to the peri-vesical fat on the T2-weighted image (A), diffusion weighted imaging (DWI) (B) and the Apparent Diffusion Coefficient (ADC) Map (C). The image of the PET fused with the T2-weighted image shows a significantly increased uptake of ^{18}F-FDG, and the SUVmax was measured as 20.95 (D). The ^{18}F-FDG PET/MR detection suggested of T3 stage. The pathological results from RC specimens revealed the T3 stage, which proved the correct staging of ^{18}F-FDG PET/MR.

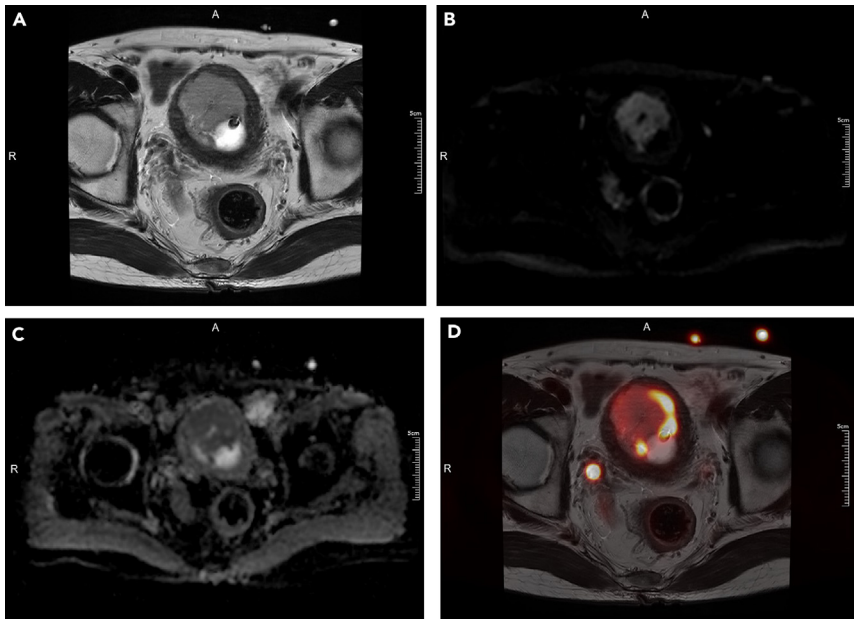

Figure 3. Pre-transurethral resection ^{18}F-FDG PET/MRI images of a 60-year-old man

(A–D) The image shows a significant and heterogeneous tumor mass, which is linked with the right anterior wall of the bladder with a pedicular connection on the T2-weighted image (A), DWI (B) and the ADC Map (C). The image of the PET fused with T2-weighted images shows a significantly increased uptake of ^{18}F-FDG, and the SUVmax was determined as 12.29 (D). The ^{18}F-FDG PET/MR detection suggested of T1 stage. The pathological results from TUR-BT specimens revealed the T1 stage, which proved the correct staging of ^{18}F-FDG PET/MR.

pain of urinary tract are more likely to belong to advanced cases. After identifying the symptoms, the patients will be evaluated by CT urography and cystoscopy to localize and find the suspected tumor lesion. When a suspected lesion is found, TUR-BT will be utilized to both verify and stage the BLCA based on the histopathological diagnosis on the resected tissue, which includes the tumoral exophytic part, the underlying bladder wall with the detrusor muscle, and the marginal edge parts of the resection area. Physical examination is also indispensable in the process of routine staging for BLCA patients, which mainly includes the rectal and vaginal bimanual palpation. In locally advanced BLCA patients, the palpable tumor mass could be found. Moreover, the bimanual examination is required to be performed before and after TUR-BT to evaluate whether the tumor mass is fixed to the pelvic wall. TUR-BT is currently the first choice for muscle invasion detection. However, TUR-BT is an invasive operation and may lead to understaging.[16,17] Therefore, noninvasive alternatives for accurate staging of BLCA are urgently warranted, and imaging is becoming increasingly important for local- and distant staging of BLCA, including MRI and CT. As with traditional imaging modalities, CT could not accurately differentiate the muscle invasion in BLCA, and both MRI and CT didn't show satisfactory sensitivity in lymph node metastasis detection.[23–25] Recently, molecular imaging has emerged as a promising imaging modality for a wide range of cancers, including BLCA. The combination of metabolic information from PET and the advantageous utility of anatomical detection of MRI is thought to complement each other and improve the staging performance for BLCA. Nevertheless, numbers of related research are relatively small. A prospective pilot study was designed to explore the value of additional PET information for the diagnosis of BLCA and found that ^{18}F-FDG-PET/MRI was helpful in improving the suspicion of tumors by MRI alone and had a higher accuracy for nodal involvement detection than MRI.[26] This study suggested a potential practical role of PET/MRI for the diagnosis of BLCA. Furthermore, in 2020, another pilot study demonstrated that ^{18}F-FDG-PET/MRI had a sensitivity of 0.80 and a specificity of 0.56 for the primary detection of BLCA,[10] which is similar with that of CT. However, limited by the low number of patients with nodal involvement, the ability of ^{18}F-FDG-PET/MRI to differentiate lymph node metastasis is still elusive. In addition to FDG, Salminen et al. evaluated the feasibility of ^{11}C-acetate PET/MRI for staging BLCA and found that the sensitivity, specificity, and accuracy for discriminating MIBC were 100%, 69% and 73%, respectively, which revealed the great practicality of ^{11}C-acetate PET/MRI in T staging BLCA. However, when it comes to the nodal involvement detection, the sensitivity of ^{11}C-acetate PET/MRI is only 0.2,[22] which demonstrated that ^{11}C-acetate may not be an ideal nuclide imaging agent for BLCA staging.

In our current study, ^{18}F-FDG PET/MRI demonstrated the sensitivity, specificity, and accuracy of 96.7%, 88.9% and 94.9%, respectively, for discriminating MIBC from NMIBC. A total of 1 in 39 patients were proven to be overstaged by ^{18}F-FDG-PET/MRI. This result is in consistency with the results of the study in 2020.[10] The main reason may be the interference of the tissue inflammation. Previous studies indicated that inflammation within tissue may cause high FDG activity, which may influence the accuracy of BLCA evaluation due to a suboptimal target-to-background ratio and this shortcoming is especially obvious in ^{18}F-FDG-PET/CT.[27,28] In comparison, MRI possesses higher contrast resolution than CT, which provides with an improved delineation of the muscularis propria of the bladder wall and thereby improved the accuracy of local staging of BLCA and avoided the influence of inflammation.[29] Meanwhile, we found that the accuracy of ^{18}F-FDG PET/MRI (94.9%) was

Table 3. Pathological and imaging results of primary tumor from enrolled participants

PT.	TUR-BT	Radical Cystectomy	PET/MR	PET/MRI results
1[a]	T2	T1N0	T3N0	TP
2[a]	T2	T1N0	T3N1	TP, FP for LN
3[a]	T2	T2N0	T3N0	TP
4[a]	T2	T3N0	T3N0	TP
5[a]	T2	T1N0	T1N0	FN for MI
6[a]	T2	T1N0	T3N0	TP
7[a]	T2	T1N0	T2N0	TP
8[a]	T2	T1N0	T2N1	TP
9[a]	T2	T2N0	T2N0	TP
10[a]	T2	T3aN0	T2N0	TP
11	T2	/	T3N0	TP
12	Ta	/	T1N0	TN
13	T2	/	T3N0	TP
14	Ta	T1N0	T1N0	TN
15	T1	T2N0	T3N0	TP
16	T2	/	T4N1	TP
17	T1	T0N0	T1N0	TN
18	T1	/	T1N1	TN
19	T2	/	T3N1	TP
20	T2	T2N0	T2N0	TP
21	T2	T3N3	T3N3	TP
22	T1	/	T1N0	TN
23	T1	/	T1N0	TN
24[a]	T2	T1N0	T3N0	TP
25	T2	/	T3N1	TP
26	T1	/	T2N0	FP for MI
27	T2	T3aN0	T3N0	TP
28	T2	/	T3N1	TP
29	T2	/	T3N0	TP
30	T1	T1N0	T1N0	TN
31[a]	T2	T3aN2	T3N1	TP
32	T2	/	T3N1	TP
33	T2	/	T3N0	TP
34[a]	T2	T2aN0	T3N0	TP
35[a]	T2	T0N0	T3N0	TP
36[a]	T2	T3aN2	T3N1	TP
37[a]	T2	/	T3N0	TP
38	T2	T2N1	T2N0	TP, FN for LN
39	Ta	/	T1N0	TN

[a]Patients receiving NAT treatment; LN: lymph node; MI: muscle invasiveness; TP: true positive; FP: false positive; TN: true negative; FN: false negative.

higher than ^{11}C-acetate (73%).[22] Theoretically, the excretion of 11C-acetate occurs through the digestive system, resulting in a relatively low radioactive retention in the urinary system, which means that the local imaging of ^{11}C-acetate in the bladder would be more effective and clearer than ^{18}F-FDG, which undergoes metabolism by the urinary system leading to extensive and undesired uptake in the residual urine within the bladder. To avoid the confounding effect of urine uptake, some researchers performed the diuresis protocol.[30,31] Based on our empirical observations, implementing stringent water intake limitations, and employing bladder irrigation prove effective in mitigating the potential interference caused by urine and attaining the desired imaging outcome. Compared with other protocols of bladder preparation, like forced

Table 4. Performance of N staging by PET/MR

Lymph node				
Gold standard from surgical specimens				
PET/MRI		Positive	Negative	In total
	Positive	4	2	6
	Negative	1	17	18
	In total	5	19	24
	Sensitivity	80%		
	Specificity	89.5%		
	PPV	66.7%		
	NPV	94.4%		
	Accuracy	87.5%		

diuresis, our bladder preparation protocol of bladder rinsing and water intake restriction exhibit some unique advantages. First, our bladder preparation protocol has good uniformity and reproducibility to ensure a relatively stable urine elimination effect. Meanwhile, the forced diuresis protocol may lead to higher heterogeneity in the efficiency of urine clearance, which resulted from the varied sensitivities and responses to the administration of diuretics. Second, the protocol of forced diuresis belongs to the medication operation, which may make the process of bladder preparation complex and lengthy. In contrast, our bladder preparation protocol is relatively simple and convenient. Moreover, the forced diuresis operation has a range of contraindications and potential drug risks, while our protocol is relatively safe. However, we still cannot neglect the limitations derived from the possible interfering of radioactive urine. As is shown in Table S1, the PET uptake of urine is still high, which determines that our bladder preparation protocol is still unsatisfactory. First, owing to the common examination position of supine position, the radioactive urine usually deposits on the posterior wall of bladder, which means that the neoplastic mass located on the posterior wall is more susceptible to the interference of the radioactive urine. The imaging overlap between the urine and tumor may decrease the accuracy of the radioactive uptake imaging of tumors and its exhibited tumoral malignancy. Also, the radioactive urine would also interfere the effective and accurate acquisition of the PET/MRI parameters. For one thing, the overlap of the urine and tumor image will change the

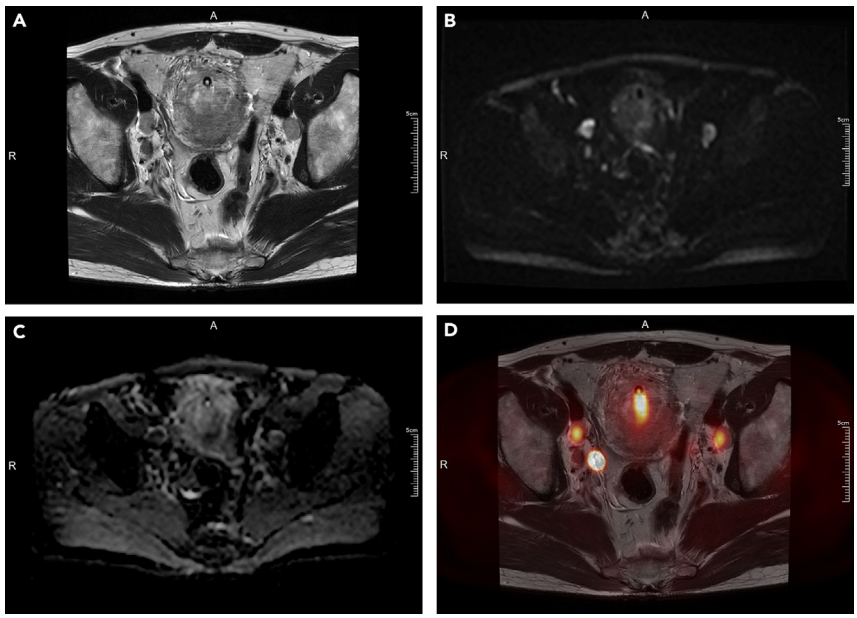

Figure 4. Pre-radical cystectomy ^{18}F-FDG PET/MRI images of a 48-year-old man

(A–D) The image shows that the bladder wall is diffusely thickened, especially in the posterior wall with abnormal signal on the T2-weighted image (A), DWI (B) and the ADC Map (C) and the tumor lesion invaded the whole bladder layer and involved the peri-vesical fat space, which indicated a typical T3 stage bladder cancer. Multiple swollen lymph nodes could be seen near the right common iliac vessels and bilateral pelvic wall iliac vessels and the diameter of the largest one reaches 1.6cm. PET fused with T2-weighted images shows a significantly increased uptake of ^{18}F-FDG in the enlarged lymph nodes, and the SUVmax was determined as 6.08 (D). The ^{18}F-FDG PET/MR detection suggested of a T3 stage bladder cancer with lymph node metastasis. The pathological results from RC specimens revealed a T3aN2 stage, which proved the correct staging of ^{18}F-FDG PET/MR.

Table 5. Correlation between PET/MRI-derived parameters and pathological characteristics of bladder cancer

	Radiological parameters			
Pathological characteristics	Diameter	ADC mean	SUVmean	SUVmax
Tumor grade				
Low	48.80(33–69)	0.866(0.615–0.992)	4.333(1.440–7.263)	5.845(2.508–9.906)
High	45.13(16–81)	0.826(0.468–1.075)	4.455(1.573–8.843)	7.733(1.843–22.139)
p value	0.6812	0.5778	0.9006	0.3380
pT stage				
T1	31.17(16–46)	0.975(0.857–1.206)	5.622(2.767–8.843)	7.014(3.337–10.254)
T2/3	51.92(18–81)	0.783(0.468–1.075)	4.988(2.110–8.544)	8.437(2.508–22.139)
p value	**0.0415***	**0.0041****	0.4375	0.4208
pN stage				
N0	42.63(12–69)	0.807(0.498–1.075)	4.573(1.440–8.843)	7.954(2.508–22.139)
N1	56.00(41–77)	0.793(0.636–1.000)	4.059(2.000–8.050)	8.787(3.302–16.497)
p value	0.1174	0.8642	0.6350	0.7201

tumoral SUVmax and SUVmean. For another, when the area of the radioactive urine is too large and the overlap part is excessive, the effective delineation of the ROI will be difficult. In all, despite that our bladder preparation protocol exhibits certain efficiency and safety, it is still far from satisfactory. Further investigations are required to achieve a better bladder preparation effect. Furthermore, it is noteworthy that a comprehensive analysis of the obtained images should be conducted through close collaboration between the team of radiologists and nuclear medicine physicians. This collaboration is crucial as radiologists possess extensive expertise in distinguishing muscle invasiveness and the anatomical structure of the bladder and neoplasm. Such collaboration significantly reduces the likelihood of erroneous judgments.

With regards to the N staging, ^{18}F-FDG-PET/MRI showed a sensitivity, specificity, and accuracy of 80%, 89.5%, 87.5%, respectively, which outperformed ^{11}C-acetate PET/MRI in 2018.[22] On the patient level, Salminen et al. found that ^{11}C-acetate-PET/MRI demonstrated a sensitivity, specificity, and accuracy of 50%, 67%, and 60% respectively, which is far from satisfactory. First, it is noteworthy that the LN metastasis evaluation of this study was only performed on 5 patients (including 2 LN + patients), of which the relatively small sample size may in part affect the final detection accuracy.[22] Second, a meta-analysis revealed that the use of ^{11}C-acetate tracer for BLCA lymph node metastasis detection

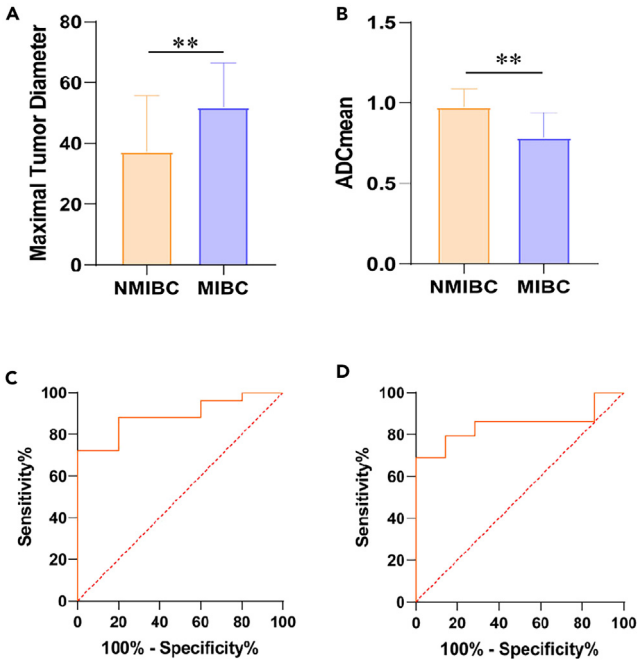

Figure 5. Correlations between PET/MR parameters of maximal tumor diameter and ADCmean and pT stage of BLCA

(A and B) Receiver operating characteristic (ROC) curves comparing the effectiveness of the PET/MR parameters for differentiating muscle-invasiveness of BLCA (C and D) (*$p < 0.05$; **$p < 0.01$; ***$p < 0.001$; ns , $p > 0.05$).

Table 6. Performance of NAT response prediction and evaluation by PET/MRI

Patient	PET/MR1	PET/MR2	RC Specimen	Response	Result
1	/	Ta N0	TisN0	positive	TP
2	T3N1	T1N1	T1N0	positive	TP (FP for LN)
3	T3N0	T1N0	T1N0	positive	TP
4	T3N0	T3N0	T3N0	negative	TN
5	T1N0	T1N0	T1N0	positive	TP
6	T2N0	T1N0	T1N0	positive	TP
7	T2N1	T1N0	T1N0	positive	TP
8	T2N0	T2N0	T2N0	negative	TN
9	T2N0	T2N0	T3aN0	negative	TN
10	T3N0	T1N0	T2aN0	negative	FP
11	T2bN0	T0N0	T0N0	positive	TP
12	T3N1	T3N1	T3N2	negative	TN
13	T3N1	T3N1	T1N0	positive	FN

NAT response

PET/MR		Positive	Negative	In total
	Positive	7	1	8
	Negative	1	4	5
	In total	8	5	13
	Sensitivity	87.5%		
	Specificity	80%		
	PPV	87.5%		
	NPV	80%		
	Accuracy	84.6%		

demonstrated a low sensitivity, which is in consistency with the ACEBIB trial, which may further verify the deficiency of the tracer of acetate in detecting LN metastasis.[32] Additionally, our study made up for the deficiency of the study in 2020[10] with no lymph node-positive patients and further improved the evaluation of lymph node metastasis by PET/MRI. Despite the demonstrated advantages of ^{18}F-FDG-PET/MRI in detecting lymph node metastasis of BLCA, we should not ignore the 3 false diagnoses, of which two are false positive and one is false negative. New means to effectively differentiate the tumor-involved lymph nodes and inflammatory enlarged lymph nodes are urgently required, which may help us avoid misdiagnosis in ^{18}F-FDG-PET/MRI for N staging. To our knowledge, our present trial is the third ^{18}F-FDG-PET/MRI study to evaluate lymph node metastasis in BLCA. Eulitt et al. reported that FDG-PET/MRI radiology revealed a sensitivity of 0% and a specificity of 100% for lymph node metastasis detection.[10] However, there was no lymph node-metastatic positive patients in that study, which largely influenced the accuracy of detection efficiency. More recently, Civelek et al. analyzed the value of ^{18}F-FDG-PET/MRI for metastatic lesions compared with CT for MIBC based on 15 patients and found that ^{18}F-FDG-PET/MRI detected nearly 30% more lymph node metastatic lesions than CT (22 vs. 17),[33] which demonstrated potential predominance of ^{18}F-FDG-PET/MRI for lymph node metastasis in BLCA. Moreover, Jenson et al. made a retrospective investigation to the feasibility of using MRI and ^{18}F-FDG-PET/CT in N staging and found that no significant difference was found between MRI and ^{18}F-FDG-PET/CT for the BLCA N staging but a slight trend of advantage of ^{18}F-FDG-PET/CT compared with MRI alone, which also indicated the value of the addition of PET information for the enhanced efficacy of N staging in BLCA. However, the population was only 18, which is too small to bring solid conclusions.[34] With regards to distant metastasis, no enrolled patient was found to be involved with distant metastasis in the ^{18}F-FDG-PET/MRI examination.

Compared to conventional staging, additional findings may be achieved by PET/MRI. Multiple studies found that PET imaging could facilitate in evaluating and predicting the tumoral immune status. Chen et al. elucidated that the ^{18}F-FDG uptake in BLCA tumor, quantified by SUVmax, is significantly associated with the PD-1 and PD-L1 expression,[35] which indicated that PET/MRI or PET/CT may be useful in predicting the immune escape status of BLCA and the subsequent optimal therapeutic strategy determination. Moreover, a range of studies have found that the metabolic parameters derived from PET imaging could significantly differentiate the HER2 expression status in breast cancer and colorectal cancer, which also suggested that PET/MRI may be used in predicting HER2 status and guiding the antibody-drug conjugate therapy for BLCA.[36,37]

To our knowledge, the present trial is the first study to investigate the feasibility of ^{18}F-FDG-PET/MRI to assist in predicting the NAT response of BLCA patients. Previously, Soubra et al. performed an analysis on the feasibility of FDG-PET/CT for predicting the response to neoadjuvant chemotherapy in BLCA patients, which demonstrated a 75% sensitivity and an 89.66% specificity for differentiating the

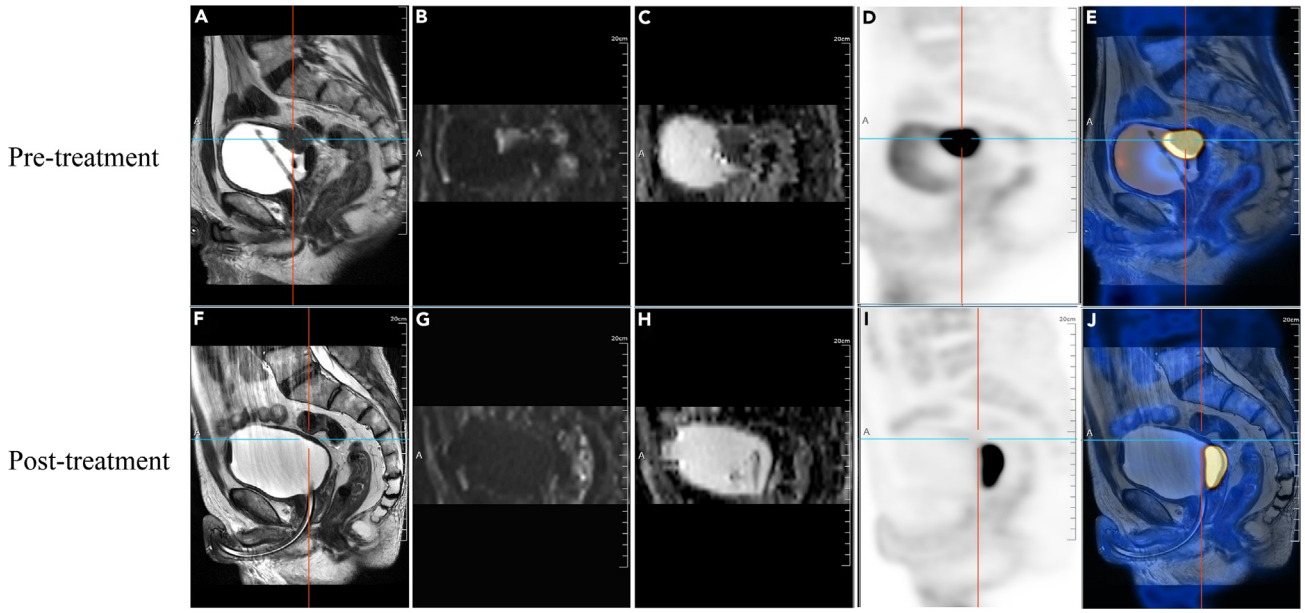

Figure 6. Comparison of bladder cancer staging (T stage) on pre-transurethral resection and post-neoadjuvant therapy ^{18}F-FDG PET/MRI in a 64-year-old male patient

A heterogeneous lobulated mass could be seen on the posterior wall of the bladder with an obvious extension to the peri-vesical fat.

(A–C) The ^{18}F-FDG uptake demonstrated a significant increase. SUVmax was determined as 27.22 and SUVmean was determined as 11.35.

(D and E) All the pre-transurethral resection ^{18}F-FDG PET/MRI images suggested a T3 stage bladder cancer. On post-neoadjuvant therapy ^{18}F-FDG PET/MRI, the mass on the posterior wall of the bladder was significantly reduced and only the local bladder wall was relatively thickened.

(F–H) FDG was slightly metabolized, and SUVmax was significantly decreased to 1.07 as detected.

(I and J) The post-neoadjuvant therapy ^{18}F-FDG PET/MRI detection suggested a T1 stage bladder cancer after the neoadjuvant therapy. The final cystectomy specimen revealed a T1 stage, thus the results of ^{18}F-PET/MRI were considered as true positive for predicting the response to neoadjuvant therapy.

patients with complete pathologic response with the 100% SUVmax reduction as an effective biomarker.[38] As for PET/MRI, Salminen et al. explored the performance of ^{11}C-acetate PET/MR for predicting the NAC response of BLCA and reported an 80% accuracy (3 in 5). However, the sample size was too small.[22] Interestingly, Fransen van de Putte et al. evaluated the accuracy of FDG-PET/CT for the response identification following neoadjuvant or induction chemotherapy (NAIC) for MIBC. Although the primary tumor downstaging could be relatively accurately distinguished from the non-response patients from non-response with an 83% sensitivity and an 80% specificity. The CR identification was less accurate with a 70% sensitivity and a 71%, which suggests that FDG-PET/CT cannot be used to select patients for RC.[39] Our present result showed that ^{18}F-FDG-PET/MR has great potential in NAT response evaluation with a satisfying accuracy (84.6%) and may serve as a useful tool for BLCA tumor restaging. In addition, we found the decrease value of SUVmean after NAT compared with the pre-NAT tumor could significantly differ the patients with good and bad response to NAT therapy. SUVmean, short for mean of standardized uptake values, is a metabolic parameter calculated by the average SUVs above a threshold of 2.5, hence it could help represent the metabolic status across the whole tumor mass.[40,41] Accordingly, SUVmean along with its changing value during treatment have been found to be able to be used for treatment efficacy prediction in multiple cancers.[42–44] However, further investigations are required to explain the inner mechanisms.

Limitations of the study

This study still has a range of limitations. First, the sample size of this study is relatively small, which may influence the accuracy and reliability of the conclusion. Second, the ^{18}F-FDG-PET/MRI-derived parameters we included in the study are not comprehensive. Owing to the technical limitations, some parameters cannot be derived, such as metabolic tumor volume (MTV) and total lesion glycolysis (TLG), and their predictive value is largely elusive. Third, this study is performed retrospectively, which may lead to selectin bias and interfere the accuracy of the conclusion. Fourth, with regards to the evaluation of the efficacy of ^{18}F-FDG-PET/MRI and its parameters in predicting NAT response in BLCA, the patients are not divided and grouped based on their PD-L1 or PD-1 expression in tumors, which may further cause the patient selection bias and negatively influence the accuracy of the conclusion.

Conclusions

In summary, our current investigation has provided evidence supporting the viability of ^{18}F-FDG-PET/MRI as an imaging modality for the clinical diagnosis of BLCA, encompassing T staging and the identification of lymph node metastasis. Additionally, we have found that

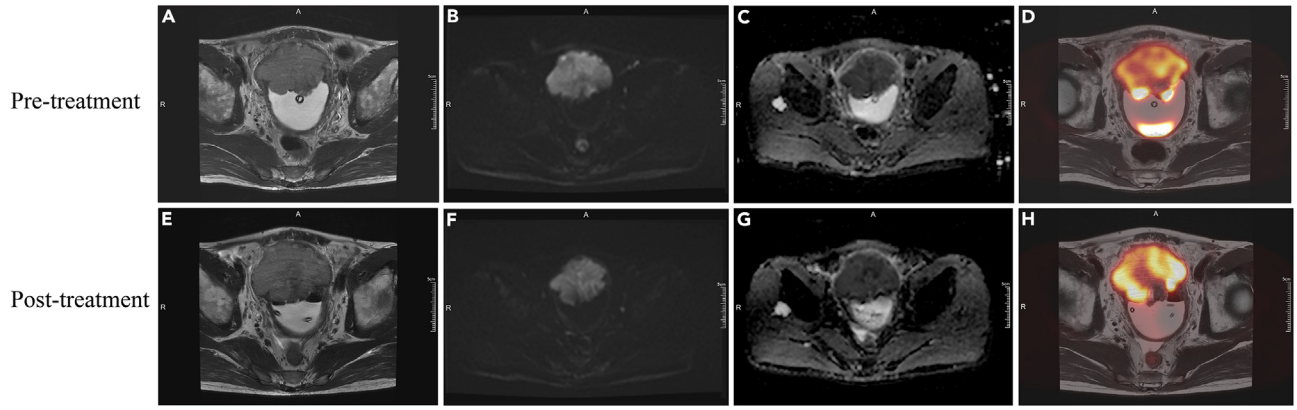

Figure 7. Comparison of bladder cancer staging (T stage) on pre-transurethral resection and post-neoadjuvant therapy ^{18}F-FDG PET/MRI in a 57-year-old male patient

A heterogeneous soft tissue mass could be seen on the anterior wall of the bladder with an extended invasion into the muscle layer and the peri-vesical fat. The size was measured as 7.7cm*5.7cm.

(A–C) The FDG uptake demonstrated a significant increase. SUVmax was measured as 19.56 and SUVmean was measured as 5.26.

(D) The pre-transurethral resection ^{18}F-FDG PET/MRI suggested a T3 stage bladder cancer. On post-neoadjuvant therapy ^{18}F-FDG PET/MRI, the previous detected mass remained on the anterior wall with the muscular and serosal invasion along with an increased size measured as 8.2cm*6.3cm (E–G), which still suggested a T3 stage. In addition, the FDG metabolism still demonstrated a high uptake value. SUVmax was measured as 15.3 and SUVmean was measured as 7.01.

(H) The post-neoadjuvant therapy ^{18}F-FDG PET/MRI detection suggested a T3 stage bladder cancer after the neoadjuvant therapy. The final cystectomy specimen revealed a T3 stage, thus the results of ^{18}F-PET/MRI were considered as true positive for predicting the poor response to neoadjuvant therapy. (*$p < 0.05$; **$p < 0.01$; ***$p < 0.001$; ns , $p > 0.05$).

^{18}F-FDG-PET/MRI, along with its derived parameter ΔSUVmean, can be utilized to effectively assess the efficacy of NAT. Specifically, the changing value of SUVmean is a good dynamic parameter for detecting the metabolic changes of tumor in face of immune-attack from NAT therapy and could be used as a promising biomarker to guide precision treatment for BLCA. However, it is recommended that future research endeavors employ larger sample sizes to validate and reinforce our discoveries.

STAR★METHODS

Detailed methods are provided in the online version of this paper and include the following:

- KEY RESOURCES TABLE
- RESOURCE AVAILABILITY
  - Lead contact
  - Materials availability
  - Data and code availability
- EXPERIMENTAL MODEL AND STUDY PARTICIPANT DETAILS
  - Participants
- METHODS DETAILS
  - ^{18}F-FDG PET/MRI examination protocol
- QUANTIFICATION AND STATISTICAL ANALYSIS

Table 7. Correlation between variation of PET/MRI-derived parameters before and after NAT and response to NAT therapy for bladder cancer patients

	Variation of radiological parameters		
	ΔDiameter	ΔSUVmean	ΔSUVmax
NAT response			
Negative	17.40(-5–52)	0.7539(-2.280-3.043)	4.197(1.110–6.156)
Positive	24.50(-5–45)	4.259(1.655–8.050)	7.420(2.183–16.497)
p value	0.5978	**0.0241***	0.1881

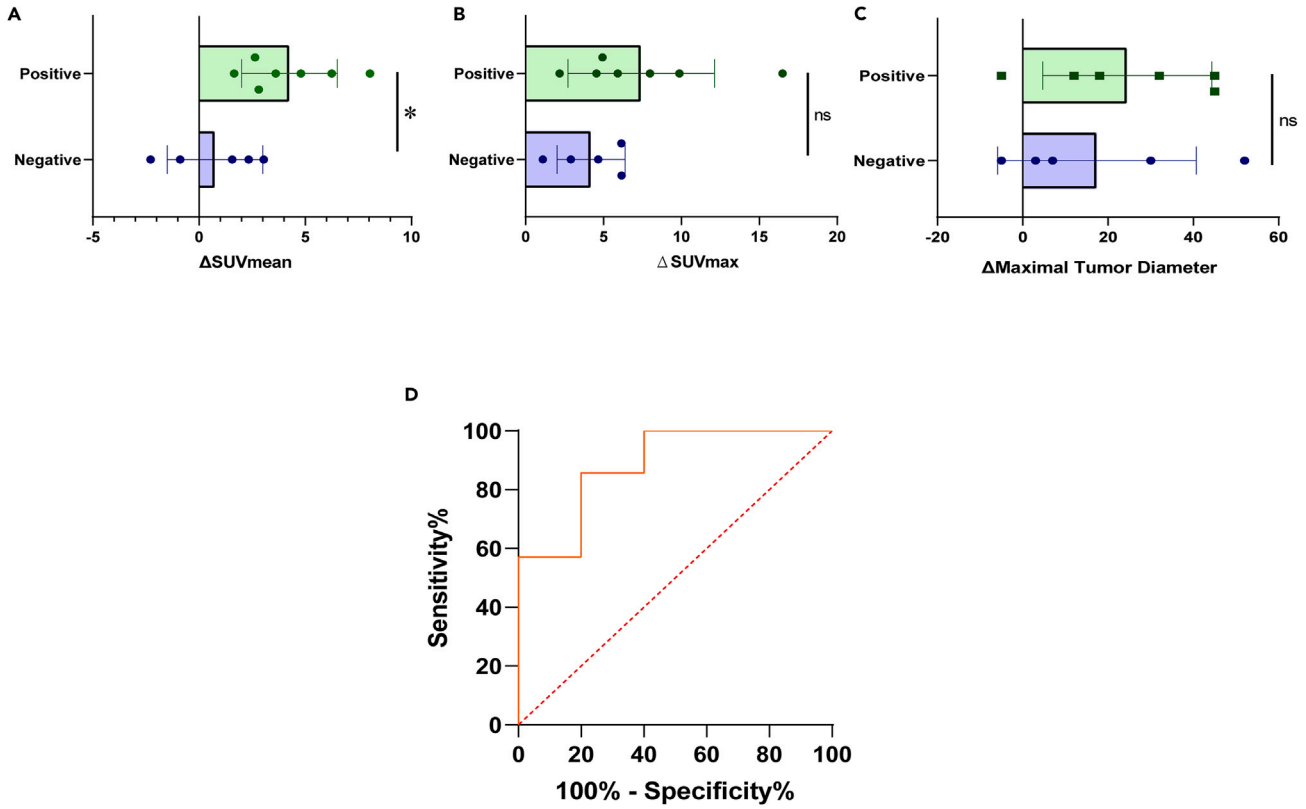

Figure 8. Efficacy of utilizing ΔSUVmean for differentiating positive-response patients of BLCA to NAT

Comparative analysis of variation of the PET/MRI parameters between positive-response and negative-response groups (A–C). Receiver operating characteristic (ROC) curves comparing the effectiveness of ΔSUVmean for differentiating positive-response patients of BLCA to NAT (D). (*$p < 0.05$; **$p < 0.01$; ***$p < 0.001$; ns , $p > 0.05$).

SUPPLEMENTAL INFORMATION

Supplemental information can be found online at https://doi.org/10.1016/j.isci.2024.109657.

ACKNOWLEDGMENTS

We thank the whole radiology and nuclear medicine team form Nanjing First Hospital and Nanjing Drum Tower Hospital for their instructions and guidance. Also, we give sincere appreciation to Figdraw (www.figdraw.com) for the assistance in the generation of the graphical abstract. This work was supported by the National Natural Science Foundation of China (82172691, and 81772710), Nanjing Science and Technology Development Key Project (YKK19011) and Fundings for Clinical Trials from the Affiliated Drum Tower Hospital, Medical School of Nanjing University (2021-LCYJ-MS-13).

AUTHOR CONTRIBUTIONS

Study concept and design: R.Y., S.A., and H.G.

Acquisition of data: T.L., Q.Y., S.Z., and R.L.

Analysis and interpretation of data: T.L., Q.Y., D.L., and S.X.

DECLARATION OF INTERESTS

The authors have declared no conflict of interest.

Received: September 7, 2023
Revised: November 19, 2023
Accepted: April 1, 2024
Published: April 3, 2024

REFERENCES

1. Siegel, R.L., Miller, K.D., Fuchs, H.E., and Jemal, A. (2021). Cancer Statistics, 2021. CA. Cancer J. Clin. *71*, 7–33. https://doi.org/10.3322/caac.21654.
2. Cathomas, R., Lorch, A., Bruins, H.M., Compérat, E.M., Cowan, N.C., Efstathiou, J.A., Fietkau, R., Gakis, G., Hernández, V., Espinós, E.L., et al. (2022). The 2021 Updated European Association of Urology Guidelines on Metastatic Urothelial Carcinoma. Eur. Urol. *81*, 95–103. https://doi.org/10.1016/j.eururo.2021.09.026.
3. Chang, S.S., Bochner, B.H., Chou, R., Dreicer, R., Kamat, A.M., Lerner, S.P., Lotan, Y., Meeks, J.J., Michalski, J.M., Morgan, T.M., et al. (2017). Treatment of Non-Metastatic Muscle-Invasive Bladder Cancer: AUA/ASCO/ASTRO/SUO Guideline. J. Urol. *198*, 552–559. https://doi.org/10.1016/j.juro.2017.04.086.
4. Redelman-Sidi, G., Glickman, M.S., and Bochner, B.H. (2014). The mechanism of action of BCG therapy for bladder cancer–a current perspective. Nat. Rev. Urol. *11*, 153–162. https://doi.org/10.1038/nrurol.2014.15.
5. Chung, J.M., Ha, H.K., Kim, D.H., Joo, J., Kim, S., Sohn, D.W., Kim, S.H., and Seo, H.K. (2017). Evaluation of the Efficacy of Solifenacin for Preventing Catheter-Related Bladder Discomfort After Transurethral Resection of Bladder Tumors in Patients With Non-Muscle Invasive Bladder Cancer: A Prospective, Randomized, Multicenter Study. Clin. Genitourin. Cancer *15*, 157–162. https://doi.org/10.1016/j.clgc.2016.05.006.
6. Cowan, N.C., and Crew, J.P. (2010). Imaging bladder cancer. Curr. Opin. Urol. *20*, 409–413. https://doi.org/10.1097/MOU.0b013e32833cbcb9.
7. Juri, H., Narumi, Y., Panebianco, V., and Osuga, K. (2020). Staging of bladder cancer with multiparametric MRI. Br. J. Radiol. *93*, 20200116. https://doi.org/10.1259/bjr.20200116.
8. Caglic, I., Panebianco, V., Vargas, H.A., Bura, V., Woo, S., Pecoraro, M., Cipollari, S., Sala, E., and Barrett, T. (2020). MRI of Bladder Cancer: Local and Nodal Staging. J. Magn. Reson. Imag. *52*, 649–667. https://doi.org/10.1002/jmri.27090.
9. Bouchelouche, K. (2022). PET/CT in Bladder Cancer: An Update. Semin. Nucl. Med. *52*, 475–485. https://doi.org/10.1053/j.semnuclmed.2021.12.004.
10. Eulitt, P.J., Altun, E., Sheikh, A., Wong, T.Z., Woods, M.E., Rose, T.L., Wallen, E.M., Pruthi, R.S., Smith, A.B., Nielsen, M.E., et al. (2020). Pilot Study of [18F] Fluorodeoxyglucose Positron Emission Tomography (FDG-PET)/Magnetic Resonance Imaging (MRI) for Staging of Muscle-invasive Bladder Cancer (MIBC). Clin. Genitourin. Cancer *18*, 378–386.e1. https://doi.org/10.1016/j.clgc.2020.02.008.
11. Joshi, M., Holder, S.L., Zhu, J., Zheng, H., Komanduri, S., Warrick, J., Yasin, H., Garje, R., Jia, B., Drabick, J.J., et al. (2022). Avelumab in Combination with Eribulin Mesylate in Metastatic Urothelial Carcinoma: BTCRC GU-051, a Phase 1b Study. Eur. Urol. Focus *8*, 483–490. https://doi.org/10.1016/j.euf.2021.03.005.
12. Funt, S.A., Lattanzi, M., Whiting, K., Al-Ahmadie, H., Quinlan, C., Teo, M.Y., Lee, C.H., Aggen, D., Zimmerman, D., McHugh, D., et al. (2022). Neoadjuvant Atezolizumab With Gemcitabine and Cisplatin in Patients With Muscle-Invasive Bladder Cancer: A Multicenter, Single-Arm, Phase II Trial. J. Clin. Oncol. *40*, 1312–1322. https://doi.org/10.1200/JCO.21.01485.
13. Grossman, H.B., Natale, R.B., Tangen, C.M., Speights, V.O., Vogelzang, N.J., Trump, D.L., deVere White, R.W., Sarosdy, M.F., Wood, D.P., Jr., Raghavan, D., and Crawford, E.D. (2003). Neoadjuvant chemotherapy plus cystectomy compared with cystectomy alone for locally advanced bladder cancer. N. Engl. J. Med. *349*, 859–866. https://doi.org/10.1056/NEJMoa022148.
14. Advanced Bladder Cancer ABC Meta-analysis Collaboration (2005). Neoadjuvant chemotherapy in invasive bladder cancer: update of a systematic review and meta-analysis of individual patient data advanced bladder cancer (ABC) meta-analysis collaboration. Eur. Urol. *48*, 202–206. https://doi.org/10.1016/j.eururo.2005.04.006.
15. Rouanne, M., Bajorin, D.F., Hannan, R., Galsky, M.D., Williams, S.B., Necchi, A., Sharma, P., and Powles, T. (2020). Rationale and Outcomes for Neoadjuvant Immunotherapy in Urothelial Carcinoma of the Bladder. Eur. Urol. Oncol. *3*, 728–738. https://doi.org/10.1016/j.euo.2020.06.009.
16. Joung, J.Y., Han, K.S., Kim, T.S., Seo, H.K., Chung, J., and Lee, K.H. (2008). Single institutional experience of bladder-preserving trimodality treatment for muscle-invasive bladder cancer. J. Kor. Med. Sci. *23*, 598–603. https://doi.org/10.3346/jkms.2008.23.4.598.
17. Packiam, V.T., and Bhindi, B. (2021). Are We Moving Closer to Accurate Restaging after Neoadjuvant Chemotherapy for Muscle-invasive Bladder Cancer? Eur. Urol. *79*, 372–373. https://doi.org/10.1016/j.eururo.2020.09.019.
18. Becker, R.E.N., Meyer, A.R., Brant, A., Reese, A.C., Biles, M.J., Harris, K.T., Netto, G., Matoso, A., Hoffman-Censits, J., Hahn, N.M., et al. (2021). Clinical Restaging and Tumor Sequencing are Inaccurate Indicators of Response to Neoadjuvant Chemotherapy for Muscle-invasive Bladder Cancer. Eur. Urol. *79*, 364–371. https://doi.org/10.1016/j.eururo.2020.07.016.
19. Wang, J., Shih, T.T.F., and Yen, R.F. (2017). Multiparametric Evaluation of Treatment Response to Neoadjuvant Chemotherapy in Breast Cancer Using Integrated PET/MR. Clin. Nucl. Med. *42*, 506–513. https://doi.org/10.1097/RLU.0000000000001684.
20. Lee, D.H., Lee, J.M., Hur, B.Y., Joo, I., Yi, N.J., Suh, K.S., Kang, K.W., and Han, J.K. (2016). Colorectal Cancer Liver Metastases: Diagnostic Performance and Prognostic Value of PET/MR Imaging. Radiology *280*, 782–792. https://doi.org/10.1148/radiol.2016151975.
21. Zhang, X., Chen, Y.L.E., Lim, R., Huang, C., Chebib, I.A., and El Fakhri, G. (2016). Synergistic role of simultaneous PET/MRI-MRS in soft tissue sarcoma metabolism imaging. Magn. Reson. Imaging *34*, 276–279. https://doi.org/10.1016/j.mri.2015.10.027.
22. Salminen, A., Jambor, I., Merisaari, H., Ettala, O., Virtanen, J., Koskinen, I., Veskimae, E., Sairanen, J., Taimen, P., Kemppainen, J., et al. (2018). ^{11}C-acetate PET/MRI in bladder cancer staging and treatment response evaluation to neoadjuvant chemotherapy: a prospective multicenter study (ACEBIB trial). Cancer Imag. *18*, 25. https://doi.org/10.1186/s40644-018-0158-4.
23. Mirmomen, S.M., Shinagare, A.B., Williams, K.E., Silverman, S.G., and Malayeri, A.A. (2019). Preoperative imaging for locoregional staging of bladder cancer. Abdom. Radiol. *44*, 3843–3857. https://doi.org/10.1007/s00261-019-02168-z.
24. Galgano, S.J., Porter, K.K., Burgan, C., and Rais-Bahrami, S. (2020). The Role of Imaging in Bladder Cancer Diagnosis and Staging. Diagnostics *10*, 703. https://doi.org/10.3390/diagnostics10090703.
25. Salmanoglu, E., Halpern, E., Trabulsi, E.J., Kim, S., and Thakur, M.L. (2018). A glance at imaging bladder cancer. Clin. Transl. Imaging *6*, 257–269. https://doi.org/10.1007/s40336-018-0284-9.
26. Rosenkrantz, A.B., Friedman, K.P., Ponzo, F., Raad, R.A., Jackson, K., Huang, W.C., and Balar, A.V. (2017). Prospective Pilot Study to Evaluate the Incremental Value of PET Information in Patients With Bladder Cancer Undergoing 18F-FDG Simultaneous PET/MRI. Clin. Nucl. Med. *42*, e8–e15. https://doi.org/10.1097/RLU.0000000000001432.
27. Pijl, J.P., Nienhuis, P.H., Kwee, T.C., Glaudemans, A.W.J.M., Slart, R.H.J.A., and Gormsen, L.C. (2021). Limitations and Pitfalls of FDG-PET/CT in Infection and Inflammation. Semin. Nucl. Med. *51*, 633–645. https://doi.org/10.1053/j.semnuclmed.2021.06.008.
28. Civelek, A.C., Niglio, S.A., Malayeri, A.A., Lin, J., Gurram, S., Chalfin, H.J., Turkbey, B., Valera, V., Steinberg, S.M., and Apolo, A.B. (2021). Clinical value of ^{18}FDG PET/MRI in muscle-invasive, locally advanced, and metastatic bladder cancer. Urol. Oncol. *39*, 787.e17–787.e21. https://doi.org/10.1016/j.urolonc.2021.04.024.
29. Nakamura, K., Joja, I., Nagasaka, T., Fukushima, C., Kusumoto, T., Seki, N., Hongo, A., Kodama, J., and Hiramatsu, Y. (2012). The mean apparent diffusion coefficient value (ADCmean) on primary cervical cancer is a predictive marker for disease recurrence. Gynecol. Oncol. *127*, 478–483. https://doi.org/10.1016/j.ygyno.2012.07.123.
30. Coquan, E., Lasnon, C., Joly, F., Lefort, J.M., and Aide, N. (2014). Diuretic ^{18}F-FDG PET/CT for therapy monitoring in urothelial bladder cancer. Eur. J. Nucl. Med. Mol. Imag. *41*, 1818–1819. https://doi.org/10.1007/s00259-014-2800-0.
31. Nayak, B., Dogra, P.N., Naswa, N., and Kumar, R. (2013). Diuretic 18F-FDG PET/CT imaging for detection and locoregional staging of urinary bladder cancer: prospective evaluation of a novel technique. Eur. J. Nucl. Med. Mol. Imag. *40*, 386–393. https://doi.org/10.1007/s00259-012-2294-6.
32. Kim, S.J., Koo, P.J., Pak, K., Kim, I.J., and Kim, K. (2018). Diagnostic accuracy of C-11 choline and C-11 acetate for lymph node staging in patients with bladder cancer: a systematic review and meta-analysis. World J. Urol. *36*, 331–340. https://doi.org/10.1007/s00345-017-2168-4.
33. Kahn Ali, S., Ait-Mohand, S., Dumulon-Perreault, V., and Guérin, B. (2021). [^{68}Ga]Ga-4HMSA a promising new PET tracer for imaging inflammation. EJNMMI Res. *11*, 114. https://doi.org/10.1186/s13550-021-00856-w.

34. Jensen, T.K., Holt, P., Gerke, O., Riehmann, M., Svolgaard, B., Marcussen, N., and Bouchelouche, K. (2011). Preoperative lymph-node staging of invasive urothelial bladder cancer with 18F-fluorodeoxyglucose positron emission tomography/computed axial tomography and magnetic resonance imaging: correlation with histopathology. Scand. J. Urol. Nephrol. *45*, 122–128. https://doi.org/10.3109/00365599.2010.544672.

35. Chen, R., Zhou, X., Liu, J., and Huang, G. (2019). Relationship between the expression of PD-1/PD-L1 and ^{18}F-FDG uptake in bladder cancer. Eur. J. Nucl. Med. Mol. Imag. *46*, 848–854. https://doi.org/10.1007/s00259-018-4208-8.

36. McGale, J., Khurana, S., Huang, A., Roa, T., Yeh, R., Shirini, D., Doshi, P., Nakhla, A., Bebawy, M., Khalil, D., et al. (2023). PET/CT and SPECT/CT Imaging of HER2-Positive Breast Cancer. J. Clin. Med. *12*, 4882. https://doi.org/10.3390/jcm12154882.

37. Yang, Z., Liu, S., Sun, Y., Xu, J., Jiang, J., Ma, X., Zhang, Y., and Song, S. (2021). 18F-FDG PET/CT metabolic parameters and HER2 expression in colorectal cancer. Neoplasma *68*, 875–881. https://doi.org/10.4149/neo_2021_200803N807.

38. Soubra, A., Gencturk, M., Froelich, J., Balaji, P., Gupta, S., Jha, G., and Konety, B.R. (2018). FDG-PET/CT for Assessing the Response to Neoadjuvant Chemotherapy in Bladder Cancer Patients. Clin. Genitourin. Cancer *16*, 360–364. https://doi.org/10.1016/j.clgc.2018.05.008.

39. van de Putte, E.E.F., Vegt, E., Mertens, L.S., Bruining, A., Hendricksen, K., van der Heijden, M.S., Horenblas, S., and van Rhijn, B.W.G. (2017). FDG-PET/CT for response evaluation of invasive bladder cancer following neoadjuvant chemotherapy. Int. Urol. Nephrol. *49*, 1585–1591. https://doi.org/10.1007/s11255-017-1637-4.

40. Lin, P., Min, M., Lee, M., Holloway, L., Forstner, D., Bray, V., and Fowler, A. (2017). Nodal parameters of FDG PET/CT performed during radiotherapy for locally advanced mucosal primary head and neck squamous cell carcinoma can predict treatment outcomes: SUVmean and response rate are useful imaging biomarkers. Eur. J. Nucl. Med. Mol. Imag. *44*, 801–811. https://doi.org/10.1007/s00259-016-3584-1.

41. Higgins, K.A., Hoang, J.K., Roach, M.C., Chino, J., Yoo, D.S., Turkington, T.G., and Brizel, D.M. (2012). Analysis of pretreatment FDG-PET SUV parameters in head-and-neck cancer: tumor SUVmean has superior prognostic value. Int. J. Radiat. Oncol. Biol. Phys. *82*, 548–553. https://doi.org/10.1016/j.ijrobp.2010.11.050.

42. Wang, C., Zhao, K., Hu, S., Huang, Y., Ma, L., Song, Y., and Li, M. (2020). A predictive model for treatment response in patients with locally advanced esophageal squamous cell carcinoma after concurrent chemoradiotherapy: based on SUVmean and NLR. BMC Cancer *20*, 544. https://doi.org/10.1186/s12885-020-07040-8.

43. Pak, K., Cheon, G.J., Kang, K.W., Chung, J.K., Kim, E.E., and Lee, D.S. (2015). Prognostic value of SUVmean in oropharyngeal and hypopharyngeal cancers: comparison with SUVmax and other volumetric parameters of 18F-FDG PET. Clin. Nucl. Med. *40*, 9–13. https://doi.org/10.1097/RLU.0000000000000613.

44. Vinogradskiy, Y., Diot, Q., Jones, B., Castillo, R., Castillo, E., Kwak, J., Bowles, D., Grills, I., Myziuk, N., Guerrero, T., et al. (2020). Evaluating Positron Emission Tomography-Based Functional Imaging Changes in the Heart After Chemo-Radiation for Patients With Lung Cancer. Int. J. Radiat. Oncol. Biol. Phys. *106*, 1063–1070. https://doi.org/10.1016/j.ijrobp.2019.12.013.

STAR★METHODS

KEY RESOURCES TABLE

REAGENT or RESOURCE	SOURCE	IDENTIFIER
Software and algorithms		
SPSS 21.0	IBM Corp, Armonk,NY, USA	www.ibm.com/support/pages/spss-statistics-210-available-download
GraphPad Prism v.6	Prism-graphpad.com	https://www.graphpad.com/scientificsoftware/prism/
Other		
PET/MRI examination instrument	Shanghai United Imaging Medical Technology Co., Ltd.	UIH uPMRI 790
clinical trial registration number for NAT efficacy evaluation cohort	Chinese Clinical Trial Registry	ChiCTR2100051298

RESOURCE AVAILABILITY

Lead contact

Further information and requests for resources and reagents should be directed to and will be fulfilled by the lead contact, RY (doctoryr@gmail.com).

Materials availability

This study did not generate new unique reagents.

Data and code availability

- The data of the pathological and PET/MRI results information of the patients could be available from the lead contact upon request.
- This study did not report any original code.
- Any additional information required to reanalyze the data reported in this paper is available from the lead contact upon request.

EXPERIMENTAL MODEL AND STUDY PARTICIPANT DETAILS

Participants

Forty patients with BLCA from Department of Urology, Nanjing Drum Tower Hospital between December 2019 and March 2022 were retrospectively enrolled for this study. The selection and inclusion criteria include: (1) Patients 18 years or older with a clinically-indicated urothelial carcinoma of the bladder scheduled to undergo a TUR-BT or radical cystectomy with pelvic lymph node dissection were eligible. (2) The successful acquisition of the tumor specimen from TUR-BT or RC and lymph nodes specimen from ePLND for tumor staging. (3) Pre-operative ^{18}F-FDG PET/MRI scan with primary BLCA tumor uptake. (4) Successful acquisition of the PET/MRI-related parameters from the PET/MRI images. All the human participants are Asian people and belong to the han ethnic group. Moreover, the selection and inclusion criteria for the NAT efficacy evaluation cohort patients additionally include: (1) The patients are required the full-cycle NAT before the surgery of RC and ePLND. (2) The patients need to undergo the ^{18}F-FDG PET/MRI after the NAT and before the RC and ePLND. Two cohorts were generated from the enrolled patients based on different research objectives. For evaluation of primary staging performance, twenty-nine patients received ^{18}F-FDG PET/MRI prior to transurethral resection of bladder tumor (TUR-BT). The extent of ePLND includes external iliac, obturator, internal iliac, presacral and common iliac LNs. For analysis of the predictive value for NAT response, thirteen of the enrolled patients with NAT underwent ^{18}F-FDG PET/MRI before RC and ePLND. Twelve patients belonged to both cohorts.

The patients in NAT efficacy evaluation cohort are derived from a registered clinical trial (ChiCTR2100051298), which was approved by the ethical committee of Medical School of Nanjing University affiliated Nanjing Drum Tower Hospital. The NAT treatment lasted for four cycles with one cycle of twenty-one days. Within one cycle, 240 mg of the PD-1 monoantibody toripalimab plus 1000 mg/m^2 mg of gemcitabine plus 70 mg/m^2 of cisplatin were administered on day 1, and 1000 mg/m^2 mg of gemcitabine was administered on day 8.

METHODS DETAILS

^{18}F-FDG PET/MRI examination protocol

Routine preparation

All the patients signed the informed consent forms and were catheterized with double- or triple-lumen catheters before examination. Before examination on the machine, bladder irrigation was conducted with sterile saline via a catheter. The purpose of bladder irrigation is to rinse

and dilute the residual urine with sterile saline in the bladder, thereby avoiding the interference of the radionuclide imaging of urine. The process of the bladder rinsing protocol includes: (1) Firstly, the sterile saline was utilized to flush the bladder through the catheter using a 50mL injector, repeating for at least four times. The flushing flow rate was controlled depending on the patient's tolerance. (2) With regards to the judgment of the timing of ending flushing, we observed and focused on the color of the bladder flushing fluid flowing out. As most BLCA patients exhibited gross hematuria, the disappearance of macroscopic hematuria and the clear and transparent color of the bladder flushing fluid were seen as a sign of the complete and successful bladder irrigation. (3) After the bladder irrigation, a total of 300mL sterile saline was injected int the bladder through the catheter and the lumen outlet was clipped to maintain the filling of the bladder, which helped to fully expose the bladder wall morphology to ensure the effective and accurate imaging. Moreover, the bladder filling after the irrigation helped to dilute the radioactive urine and subsequently avoid the possible interference with the tumor imaging. On the day of examination, all patients were fasted and water-deprived for 6 h, and the blood glucose level was controlled below 11.1 mmol/L. Intravenous injection of ^{18}F-FDG was given according to the standard of 0.09–0.21 mCi/kg (3.33 MBq-7.77 After 40 to 60 min of quiet rest, PET/MRI examination was performed for whole body and pelvic local imaging (Shanghai United Imaging Medical Technology Co., Ltd. UIH uPMRI 790). Drinking water was strictly forbidden during rest to reduce urine storage in the bladder.

Image acquisition

The flow chart of the study is illustrated in Figure 1. During the process of full-body scanning, the patients were maintained in a supine position. The MRI attenuation correction sequence and PET acquisition started simultaneously. MRI whole-body scanning was conducted under the whole-body PET/MRI protocol, including the whole-body three-dimensional gradient echo T1-weighted imaging sequence (in-phase, anti-phase, water imaging, fat imaging), covering from head to mid-thigh, and whole-body transverse axis fast spin echo T2-weighted imaging fat suppression sequence, diffusion weighted sequence, brain three-dimensional T1WI sequence, brain three-dimensional T2-weighted fluid attenuation inversion recovery sequence. During pelvic scanning, MRI acquisition included T2WI transverse, sagittal and coronal high-resolution sequences, T2WI transverse and coronal fat suppression sequences, T1WI transverse high-resolution sequences, and diffusion weighted sequences (b values are 50 s/mm^2, 1000 s/mm^2 and 1500 s/mm^2, respectively). Image reconstruction was completed using time of flight (TOF) technology. The maximum expected value iteration method for ordered subsets was selected. After the scanning process, the PET/MRI fusion image was automatically reconstructed by the postprocessing workstation.

^{18}F-FDG PET/MRI image analysis

Two radiologists conducted the double-blind reading and evaluation of PET/MRI images. When the diagnostic results were inconsistent, an experienced superior nuclear medicine physician specializing in urinary system imaging was consulted. The diagnosis was made until agreement was reached. For every tumor lesion, the region of interest (ROI) was delineated on the continuous axial fusion image, and the SUVmax and SUVmean of each tumor were measured. To accurately identify the ROI, the location, scope, and the invasion extent of the primary tumor lesion are required to be firstly evaluated and confirmed comprehensively. Based on the review of the T1WI, T2WI, and DWI images, the areas of necrosis, cystic transformation, and bleeding were differentiated and avoided. Afterward, the delineation of ROI was performed based on the substantial portion of the primary lesion on the ADC image and the ADC value was measured. On the ADC image, three circular ROIs were delineated in the solid part of the lesion that can distinguish signal differences through visual analysis. The area of the delineated ROI was ensured as 0.5 cm^2 when the tumor area in the horizontal axis is sufficient. The maximal diameter of tumor foci was measured on T2WI coronal, sagittal, and horizontal axes, and the maximum was taken as the maximal tumor diameter. The ADC values of the tumor were measured on the apparent diffusion coefficient (ADC) chart (b = 1500 s/mm^2) in 3 locations with certain differences, and their mean value was taken as the mean ADC (ADCmean). The ROI was placed in the shape of a circle at the site to be measured, and the area was ensured to be 0.5 cm^2 when there was sufficient loci scope.

QUANTIFICATION AND STATISTICAL ANALYSIS

In the purpose of evaluating the feasibility of ^{18}F-FDG PET/MRI in staging BLCA, the histopathological results from TUR-BT and RC accompanied by ePLND were taken as the gold standard. For evaluation of lymph node involvement, pathologic results from biopsy or lymph node dissection served as the gold reference. If no pathologic reference standard was available or the results were influenced by NAT therapy, then either progressive nodal enlargement on serial examinations or a decrease in size during the process of NAT was considered an indicator of nodal metastasis. The sensitivity, specificity and accuracy were calculated for the detection of muscle invasion and nodal involvement. Receiver operating characteristic curve (ROC) analysis was also used to evaluate the ability of ^{18}F-FDG PET/MRI for BLCA staging. To evaluate the value of ^{18}F-FDG PET/MRI-derived parameters in staging and NAT efficacy prediction, the derived parameters were compared with subgroups of different pathological characteristics of BLCA patients by Student's t test or Mann–Whitney U test according to normality test. ROC analysis was also utilized to assess the efficacy of different parameters to differentiate distinct pathological characteristics of BLCA. Statistical analysis was performed by SPSS 21.0 (IBM Corp., Armonk, NY, USA) and GraphPad Prism v.6 (Prism-graphpad.com). p value <0.05 was viewed as significantly different.